OPTIMAL SENSOR PLACEMENT FOR DAMAGE DETECTION BASED ON A NEW GEOMETRICAL VIEWPOINT

S. Beygzadeh[1], E. Salajegheh[2,*,†], P. Torkzadeh[2], J. Salajegheh[2] and S.S. Naseralavi[2]
[1] *Department of Civil Engineering, Kerman Graduate University of Technology, Kerman, Iran*
[2] *Department of Civil Engineering, Shahid Bahonar University of Kerman, Kerman, Iran*

ABSTRACT

In this study, efficient methods for optimal sensor placement (OSP) based on a new geometrical viewpoint for damage detection in structures is presented. The purpose is to minimize the effects of noise on the damage detection process. In the geometrical viewpoint, a sensor location is equivalent to projecting the elliptical noise on to a face of response space which is corresponding to the sensor. The large diameters of elliptical noise make the damage detection process problematic. To overcome this problem, the diameters of the elliptical noise are scaled by filter factor to obtain an elliptical called equivalent elliptical noise. Based on the geometrical viewpoint, six simple forward algorithms are introduced to find the OSP. To evaluate the merits of the proposed method, a two-dimensional truss, under both static and dynamic loads, is studied. Numerical results demonstrate the efficiency of the proposed method.

1. INTRODUCTION

All engineering structures are especially susceptible to random vibrations, whether they are due to large ground accelerations, strong wind forces, or abnormal loads such as explosions

---
* Corresponding author: E. Salajegheh, Departement of Civil Engineering, Shahid Bahonar University of Kerman, Kerman, Iran
† E-mail address: eysasala@mail.uk.ac.ir

[1]. Research activities have concentrated on making use of the important technological advances in sensing and communication technology to raise safe measures in these structures. Structural health monitoring (SHM) research represents the integration domain of these efforts striving to enhance the safety and extend the service life of infrastructures [2]. In general, an SHM system includes three major components: a sensor system, a data processing system, and a health evaluation system [3]. Since a large number of sensors are involved in an SHM system, it is challenging to optimally arrange sensors strategically in a large structure in order to obtain data from those locations which will result in the best identification of structural characteristics [4]. The problem of OSP on structure arises from the following considerations: using a small number of sensors in order to reduce the cost of instrumentation and data processing; obtaining good appraises of model parameters from noisy data; improving structural control by using valid models; determining the structural properties for health monitoring of structure efficiently; and ensuring visibility of modeling errors [5]. Finding the optimal sensor locations for a structure which has a smaller number of degrees of freedom (DOF), the experience and a trial-and-error approach may suffice to solve the problem. For a large-scale structure, whose finite element (FE) model may have tens of thousands of DOFs a systematic approach is needed to solve such a computationally demanding problem [4]. Many authors have researched the OSP in the past few years. Yi et al. [4] used a generalized genetic algorithm (GGA) to optimize sensors location and compared it with that of the existing genetic algorithm. The results showed that the GGA obtained the better placement scheme. Lie et al. [6] introduced an improved genetic algorithm to find the optimized location of sensors. The result shows that it improves convergence of the algorithm. Li et al. [7] used the OSP for measurement of structure vibration and introduced an efficient method based on the uniform design method for sensor placement optimization. Worden and Burrows [8] used a neural network for OSP. Kang et al. [9] used a combination algorithm (VEPGA) which combined a partheno-genetic algorithm (PGA) with virus evolutionary theory for sensor placement optimization on a large space structure for modal identification detection. Three performance indices for sensor placement optimization (one aiming at the maximization of linear independence, another aiming at the maximization of modal energy, and the last one being a combination of the front two indices) have been investigated. The algorithm is applied to a portal frame and a concrete arc dam. The result showed that the VEPGA performance index makes a superior compromise between the linear independence aimed index and the modal energy aimed index. Sanchez-Montanes and Pearce [10] discussed how Fisher information matrix (FIM) is used for sensor placement optimization. They introduced OSP within a population to maximize the accuracy of the overall sensory system. Singh and Joshi [11] discussed that error in damage classification associated with strain pattern requires an optimum number and position for strain sensors which obtain most appropriate strain pattern that produces a minimum error of damage classification. A genetic algorithm is developed and the method applied to SHM. Shah and Udwadia [12] introduced the optimally positioning sensors in lumped and distributed parameter dynamic system as a suitable norm of the covariance matrix is minimized. The efficiency of this method, for the structure as a shear structure model that has been under strong vibration of the earth, has been demonstrated. Naseralavi et al. [13] presented an improved genetic algorithm and sensitivity analysis for fault

detection. Bakhtiari-Nejad et al. [14] introduced OSP based on FIM. Numerical results for a plane truss demonstrate the ability of this method in damage detection. Papadimitriou [15] introduced two object functions for OSP using information entropy and showed that the lower and upper bounds of information entropy are the decreasing functions of the number of sensors. Based on this result, two algorithms are proposed. The theoretical developments and the effectiveness of the proposed algorithms are illustrated by designing the optimal formation for a 10 DOFs chain-like spring-mass model and a 240 DOFs three-dimensional truss structure. Guo et al. [16] used the damage detection for objective function in optimization sensor locations using genetic algorithm for SHM. The use of statistical objective function in OSP for SHM has been quite common [17, 18]. Perez and Behdinan [19] discussed particle swarm optimization (PSO) algorithm for OSP. Improvement in the results is shown by changing the parameters and functions problems and it shows that this algorithm found better positions for sensors.

In this study, six simple forward algorithms based on a new geometrical viewpoint are proposed for OSP. Due to noisy data received by the sensors, some diameters of elliptical noise in damage space are large, so damage detection process is not exact. For scaling the elliptical noise, a new filter factor is proposed. Regularizing elliptical is called equivalent elliptical. Optimal locations for sensors obtained in two states, one using the elliptical noise before regularization, another using the equivalent elliptical noise based on geometrical viewpoint in the algorithms. The damage is detected using the recording responses from the obtaining optimal locations for sensors. The obtained results are compared to finding the best algorithm. This paper is organized as follows: Summary of sensitivity analysis for damage detection discussed in Section 2. The geometrical viewpoint for OSP described in Section 3.1. The equivalent elliptical noise described in Section 3.2. The proposed forward algorithms are presented in Section 4 and then two illustrative case studies are considered in Section 5. Finally, the conclusions end the paper in Section 6.

2. DAMAGE DETECTION USING SENSITIVITY ANALYSIS

In this research, the mathematical expression of fault detection problem can be defined by the Eq. (1).

$$\mathbf{R}_d = \mathbf{R}(\mathbf{X}) \tag{1}$$

$$\mathbf{X} = \{x_1 ,\ x_2 ,\ \cdots ,\ x_n\}^T \qquad 0 \le x_i \le 1 \tag{2}$$

where $\mathbf{X}$ is called the damage vector and n is the number of structural elements. The values $x_i = 0$ and $x_i = 1$ indicate the undamaged and completely damaged state, respectively. $\mathbf{R}_d = \{r_{d1},\ r_{d2},\ ...,r_{dm}\}^T$ is the vector of structure responses obtained from the existing damage structure and $\mathbf{R}\ (\mathbf{X}) = \{r_1(\mathbf{X}),\ r_2(\mathbf{X}),\ ...,\ r_m(\mathbf{X})\}^T$ is the vector of m responses of a hypothetically damaged structure that can be evaluated from the analytical model.

For solving the system of nonlinear equations in Eq. (1) the Taylor expansion of $\mathbf{R}\ (\mathbf{X})$ is used according to Eq. (3).

$$\mathbf{R}_d = \mathbf{R}_h + \frac{\partial \mathbf{R}}{\partial \mathbf{X}} \Delta \mathbf{X} + \ldots \tag{3}$$

where $\mathbf{R}_h$ is the response vector of healthy structure. Using the first order approximation Eq. (1) can be expressed as follows:

$$\Delta \mathbf{R} = \mathbf{R}_d - \mathbf{R}_h = \frac{\partial \mathbf{R}}{\partial \mathbf{X}} \Delta \mathbf{X} \quad , \quad \mathbf{S} = \frac{\partial \mathbf{R}}{\partial \mathbf{X}} => \Delta \mathbf{R} = \mathbf{S} \ \Delta \mathbf{X} \tag{4}$$

$$\Delta \mathbf{R} = \mathbf{S} \ (\mathbf{X} - \mathbf{X}_0) \tag{5}$$

$\mathbf{X}_0$ is the response vector of healthy structure, so it has the value of zeros. $\mathbf{S}$ is the sensitivity matrix obtained from using Equations (6) and (7) [13].

$$\mathbf{S} = \frac{\partial \mathbf{R}}{\partial \mathbf{X}} = [\ \mathbf{S}_1 \ \ \mathbf{S}_2 \ \ \mathbf{S}_3 \ \ \ldots \ \ \mathbf{S}_l \ \ \ldots \ \ \mathbf{S}_n \ ] \tag{6}$$

$$\mathbf{S}_l = \frac{\mathbf{R}_h - \mathbf{R}_{dl}}{0.001} \tag{7}$$

where $\mathbf{R}_{dl}$ is the response vector of structure when the amount of damage at lth element is 0.1% (in this study, damaging is considered as reduction in elasticity modules of the elements).

The sensitivity matrix for a damped structure system under general excitation is as follows:

$$\mathbf{S} = \begin{bmatrix} \mathbf{S}_1 \\ \mathbf{S}_2 \\ \vdots \\ \mathbf{S}_i \\ \vdots \\ \mathbf{S}_m \end{bmatrix} \quad with \quad \mathbf{S}_i = \begin{bmatrix} \dfrac{\partial \mathbf{a}_i(t_1)}{\partial x_1} & \dfrac{\partial \mathbf{a}_i(t_1)}{\partial x_2} & \ldots & \dfrac{\partial \mathbf{a}_i(t_1)}{\partial x_n} \\ \dfrac{\partial \mathbf{a}_i(t_2)}{\partial x_1} & \dfrac{\partial \mathbf{a}_i(t_2)}{\partial x_2} & \ldots & \dfrac{\partial \mathbf{a}_i(t_2)}{\partial x_n} \\ \vdots & \vdots & & \vdots \\ \dfrac{\partial \mathbf{a}_i(t_{nt})}{\partial x_1} & \dfrac{\partial \mathbf{a}_i(t_{nt})}{\partial x_2} & \ldots & \dfrac{\partial \mathbf{a}_i(t_{nt})}{\partial x_n} \end{bmatrix} \tag{8}$$

where $\mathbf{a}_i$ is the acceleration response vector with size $nt \times 1$ at the ith DOF (sensor placement) of the structure. nt is the number of data point. Matrix $\mathbf{S}_i$ with the size of $nt \times n$ is also a function of time. Since the relationship between the acceleration responses $\mathbf{a}_i$ and the fractional damage value x is nonlinear, a nonlinear model updating method, like the Gauss-Newton method, is required [20].

$\Delta \mathbf{X}$ is the damage vector change and can be determined as follows:

$$\Delta \mathbf{X} = \mathbf{S}^+ \ \Delta \mathbf{R} \tag{9}$$

The pseudo-inverse of $\mathbf{S}$ (i.e. $\mathbf{S}^+$) can be by singular value decomposition [21].

3. THEORIES

3.1. Geometrical viewpoint

The responses recorded by the sensors are noisy. The noise has a multivariate normal distribution and it is indicated as follow:

$$\boldsymbol{\varepsilon} \ \sim \ \mathbf{N}(\boldsymbol{\mu}, \Sigma) \tag{10}$$

where $\boldsymbol{\varepsilon}$ is the vector of random variable, $\boldsymbol{\mu}$ is the mean vector and Σ is the covariance matrix. Geometrically, a normal distribution interpreted as the elliptical where the eigenvalues of covariance matrix are the diameters value and mean vector is the center of this elliptical. The normal distribution for additive and multiplicative noise is as Eq. (11) and Eq. (12), respectively.

$$\mathbf{R} + \boldsymbol{\varepsilon} \ \sim \ \mathbf{N}(\mathbf{R} + \boldsymbol{\mu}, \Sigma) \tag{11}$$

$$\mathbf{R}\,\boldsymbol{\varepsilon} \ \sim \ \mathbf{N}(\mathbf{R}\,\boldsymbol{\mu}, \ \mathbf{R}\Sigma\mathbf{R}^T) \tag{12}$$

In the additive noise, Σ matrix is the diagonal. When the components on main diameter from this matrix are similar, the noise is viewed as spherical in Euclidean space. The distribution noise with unit covariance matrix is as unit spherical. In the multiplicative noise, Σ is the complete matrix, so it is viewed as elliptical in Euclidean space.

The noise is applied to Eq. (5) as follows:

$$\mathbf{S}\,\mathbf{X} = \Delta\mathbf{R} + \boldsymbol{\varepsilon} \tag{13}$$

The damage vector, $\mathbf{X}$, can be determined as follows:

$$\mathbf{X} = \mathbf{S}^+\Delta\mathbf{R} + \mathbf{S}^+\boldsymbol{\varepsilon} \tag{14}$$

The normal distribution has zero mean, $\boldsymbol{\mu} = \mathbf{0}$, and according to Eq. (12), the normal distribution for $\mathbf{S}^+\boldsymbol{\varepsilon}$ is:

$$\mathbf{S}^+\boldsymbol{\varepsilon} \ \sim \ \mathbf{N}(\mathbf{0}, \mathbf{S}^+ \Sigma \mathbf{S}^{+T}) \tag{15}$$

Geometrically, the damage vector, $\mathbf{X}$, and the response vector change, $\Delta\mathbf{R}$, are members of n-dimensional and m-dimensional Euclidean spaces, respectively. According to Eq. (14), the additive noise in response space is mapped to the damage space by matrix $\mathbf{S}^+$ and it is

changed to the multiplicative noise with covariance matrix $\mathbf{S}^+ \sum \mathbf{S}^{+T}$, according to Eq. (15). The eigenvalues of this covariance matrix are the diameters of the elliptical noise in damage space. In the present geometrical viewpoint, the noise is assumed unit spherical with covariance matrix $\mathbf{I}_{n \times n}$ in damage space and it is mapped to the response space by matrix $\mathbf{S}$ and it is changed to elliptical noise with covariance matrix $\mathbf{SS}^T$. The idea is schematically illustrated in Figure 1. In this figure, the mapping of the response space to the damage space is called "direct mapping" and the overhand is called "inverse mapping".
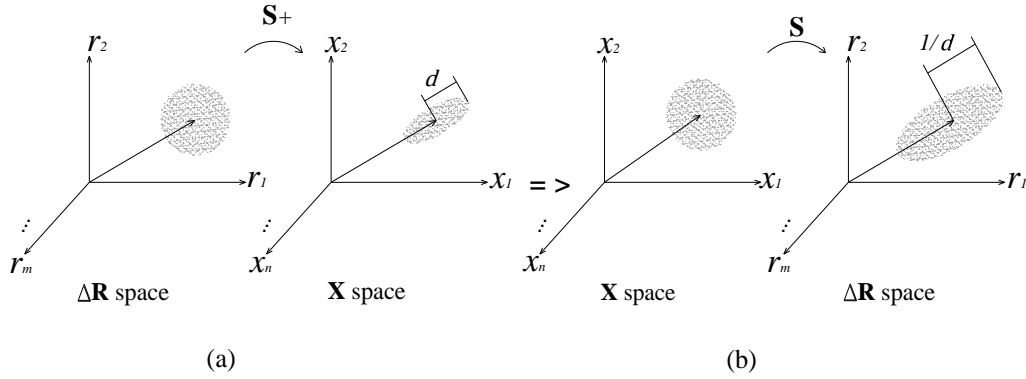

Figure 1. The geometrical interpretation: (a) Direct mapping (b) Inverse mapping

According to Figure 1, if d is the diameter of elliptical noise in direct mapping, then it is $1/d$ in inverse mapping. Therefore, the elliptical noise in response space should be large so that the noise in damage space would be small. In this viewpoint, the selection of the optimal location for sensor is viewed as the projection of the elliptical noise on the faces of response space according to Figure 2.
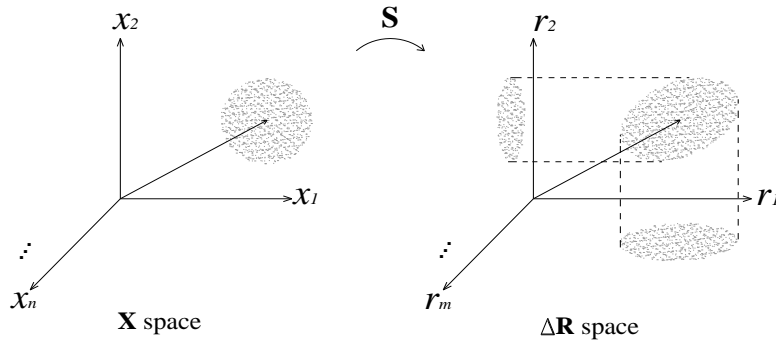

Figure 2. The projection of elliptical noise on faces of response space

For example, the aim is to find the optimal placements for three sensors in the structure with 10 DOFs. The projections of elliptical noise obtained on all faces of response space. The results show that the projections on faces r_3, r_7 and r_8 are larger than other faces. Any face is according to one sensor placement, so the sensors should be placed in DOFs 3, 7 and 8.

Generally, the noise is multiplicative in response space. In inverse mapping, the elliptical noise in damage space changes to elliptical noise in response space, so the basic assumption

is rejected in the geometrical viewpoint. To address this problem, the elliptical noise in response space is mapped to an *m*-dimensional Euclidean space by **P** matrix and changed to unit spherical noise, according to Figure 3. The definition of matrix **P** is according to Eq. (16).

$$\mathbf{P} = \begin{bmatrix} \dfrac{1}{r_{h1}} & & 0 \\ & \ddots & \\ 0 & & \dfrac{1}{r_{hm}} \end{bmatrix}$$

(16)

In Eq. (16), the vector of structure responses obtained from the existing damage structure, r_d, isn't accessible, so response vector change is approximately considered as the response vector of healthy structure *(r_{hi}- r_{di}~ r_{hi})*. Consequently, the unit spherical noise in the response space is mapped to the damage space by pseudo-inverse of **PS** as shown in Figure 3. According to the geometrical theory the unit spherical noise in damage space is mapped to response space by **PS** and it is changed to the elliptical noise with covariance matrix **PS**(**PS**)^T.
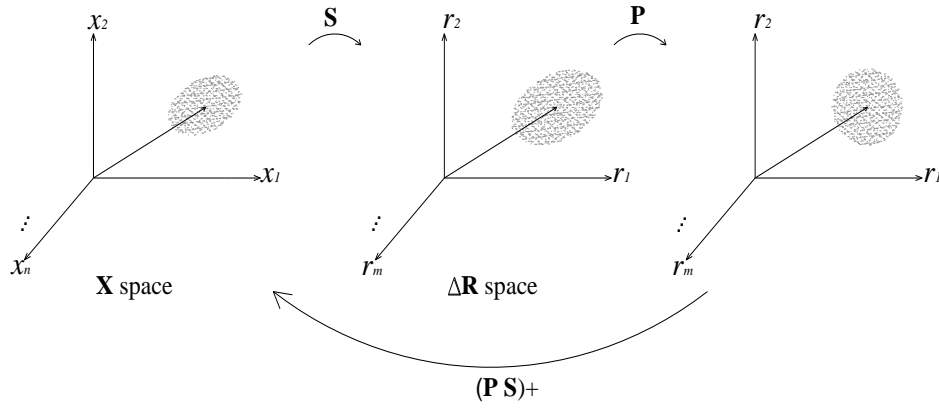
Figure 3. The elliptical noise conversion to the spherical noise

The singular value decomposition (SVD) is another method for obtaining the diameters of elliptical noise in response space. The SVD is applied on matrix **PS** with $m \times n$ ($m > n$) dimension as follows:

$$\mathbf{PS} = \mathbf{U}\sum\mathbf{V}^T = [\mathbf{u}_1 \quad \cdots \quad \mathbf{u}_n] \begin{bmatrix} \delta_1 & & 0 \\ & \ddots & \\ 0 & & \delta_n \end{bmatrix} \begin{bmatrix} \mathbf{v}_1^T \\ \vdots \\ \mathbf{v}_n^T \end{bmatrix} = \sum_{i=1}^n \delta_i \mathbf{u}_i \mathbf{v}_i^T$$

(17)

where **U** and **V** are $m \times n$ and $n \times n$ matrices, respectively; the vectors in **U** and **V** are the

direction of diameters from elliptical and spherical noises, respectively. The diagonal matrix $\sum$ contains the singular values, which are non-negative and, by convention, are numbered in descending order: $\delta_1 \geq \delta_2 \geq \dots \geq \delta_n \geq 0$. δ_i which are the diameters value of elliptical noise in response space [21].

3.2. Equivalent elliptical: regularized elliptical noise

Most damage detection methods cannot tolerate the influence of measurement errors and damage detection is not exact. The solution of Eq. (9) is often ill-conditioned and some diameters of elliptical noise are large in damage space, so regularization techniques are needed to provide bounds to the solution. The most widely used regularization method is Tikhonov regularization [20]. In this method, the optimal parameter, λ, is selected for regularization. The regularized solution can be written in the following from as,

$$\Delta \mathbf{X} = \sum_{i=1}^{m} f_i \frac{\mathbf{U}_{1i}^T \Delta \mathbf{R}}{\sigma_i} \mathbf{V}_{1i} \tag{18}$$

where $\mathbf{U}_1$, $\mathbf{V}_1$ and σ_i are obtained from applying SVD to the sensitivity matrix and f_i are referred to as filter factors which can be expressed by Eq. (19).

$$f_i = \frac{\sigma_i^2}{(\sigma_i^2 + \lambda^2)} \qquad (i = 1, 2, \dots, m) \tag{19}$$

In this study, the filter factors, h_i, for regularization of elliptical noise diameters are proposed as:

$$h_i = \frac{\left(\dfrac{1}{\gamma_i}\right)^2}{\lambda^2 + \left(\dfrac{1}{\gamma_i}\right)^2} \tag{20}$$

In Eq. (20), diameters of the elliptical noise in damage space, γ_i, are singular values on the diagonal of covariance matrix obtained from applying SVD to matrix $(\mathbf{PS})^+$. In Eq. (20) if λ is too large, then the problem solved will deviate from the main problem and if λ is too small, then the problem will be too close to the main ill-posed problem. Therefore a limitation is required on the range of λ, i.e. *min* (γ_i) $\leq \lambda \leq$ *max* (γ_i).

After regularization, the elliptical noise center is displaced according to Figure 4. The damage vector $\mathbf{X}$ changes to $\mathbf{Y}$ vector by regularization and the displacement vector of elliptical noise center, $\mathbf{D}$, will be the following form.

$$\mathbf{D} = \mathbf{Y} - \mathbf{h}\mathbf{X} \tag{21}$$

According to the theory of parallel axes, the standard deviation for elliptical noise diameters after regularization is as Eq. (22). Since the elliptical noise is composed of contours of a multivariate normal distribution, it isn't considered as the effect of area.

$$F(\lambda) = \sqrt{\left(h_1 \times \gamma_1\right)^2 + \left(h_2 \times \gamma_2\right)^2 + ... + \left(h_n \times \gamma_n\right)^2} + \left|\mathbf{D}\right|^2 \qquad (22)$$

The regularization parameter λ is determined by minimizing Eq. (22). In the following studies, the golden section method is used for determining the parameter λ.
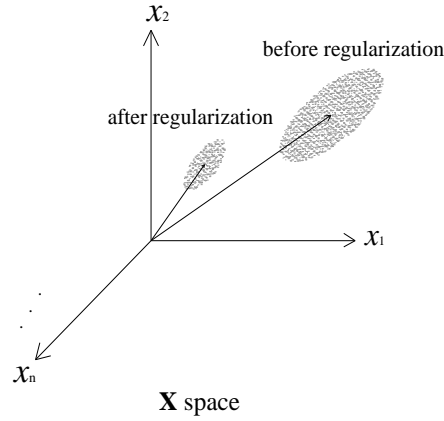

Figure 4. Center displacement of the elliptical noise after regularization

4. THE PROPOSED ALGORITHMS

Using geometrical viewpoint, six simple forward algorithms are proposed for OSP as follows:

4.1. Algorithm A

The unit spherical noise, $\mathbf{I}_{n \times n}$, in the damage space is mapped to the response space by matrix $\mathbf{PS}$ and change to elliptical noise with covariance matrix $(\mathbf{PS})\,\mathbf{I}\,(\mathbf{PS})^T = \mathbf{PS}(\mathbf{PS})^T$. The projection of this elliptical noise on the face e_i of response space (i.e. $\mathbf{e}_i \in \mathbf{R}^m$) obtained using Eq. (23).

$$proj_{\mathbf{e}_i}\mathbf{PS}(\mathbf{PS})^T = \mathbf{e}_i\mathbf{e}_i^+\mathbf{PS}(\mathbf{PS})^T \qquad (23)$$

Vector $\mathbf{e}_i$ has the size of $m \times 1$ with unit ith component and zeros elsewhere. Every vector of the response space is corresponding to a sensor placement. The optimal placements for sensors are the freedom degrees corresponding to the faces that F_A is larger in Eq. (24).

$$F_A = \left|proj_{\mathbf{e}_i}\mathbf{PS}(\mathbf{PS})^T\right| \qquad (24)$$

4.2. Algorithm B

The definition of PS_{ij} is according to Eq. (25),

$$
\mathbf{PS} = \begin{bmatrix} \dfrac{1}{r_{h1}} & & 0 \\ & \ddots & \\ 0 & & \dfrac{1}{r_{hm}} \end{bmatrix} \begin{bmatrix} \dfrac{\partial r_1}{\partial x_1} & \dfrac{\partial r_1}{\partial x_2} & \cdots & \dfrac{\partial r_1}{\partial x_n} \\ \dfrac{\partial r_2}{\partial x_1} & \dfrac{\partial r_2}{\partial x_2} & \cdots & \dfrac{\partial r_2}{\partial x_n} \\ \vdots & \vdots & \vdots & \vdots \\ \dfrac{\partial r_m}{\partial x_1} & \dfrac{\partial r_m}{\partial x_2} & \cdots & \dfrac{\partial r_m}{\partial x_n} \end{bmatrix} \Rightarrow PS_{ij} = \dfrac{1}{r_{hi}} \dfrac{\partial r_i}{\partial x_j} \qquad (25)
$$

Every row of matrix **PS** is according to a sensor location. The *i*th row with the large value for Eq. (26) is corresponding to OSP because it is corresponding to the face with large projection of elliptical noise. F_{Bi} is obtained for all rows and arranged in a decreasing order and the freedom degrees corresponding to the rows are the optimal locations for sensors, respectively.

$$
F_{Bi} = \sum_{j=1}^{n} \left| PS_{ij} \right| \qquad (26)
$$

4.3. Algorithm C

Geometrically, when the sensors are placed in optimal locations, the elliptical noise in response space is large. In other word, standard deviation has maximum value for diameters of elliptical noise in Eq. (27).

$$
F_C = \sqrt{\delta_1^2 + \delta_2^2 + ... + \delta_m^2} \qquad (27)
$$

In Eq. (27) δ_i are the diameters of elliptical noise in response space. The response space is transferred to the damage space by matrix **PS** and obtained subspace $\mathbf{PS(PS)}^+$. The elliptical noise in response space is transferred to subspace and the elliptical noise with covariance matrix $(\mathbf{PS(PS)}^+).(\mathbf{PS(PS)}^T).(\mathbf{PS(PS)}^+)^T$ obtained. Eigen values of this covariance matrix are the diameters of elliptical noise in the response space.

The basic assumption in this algorithm is that every degree of freedom has a sensor and a sensor is removed in every step of this algorithm. It means that, in every step one degree of freedom is eliminated in calculating matrix **PS**. The degree of freedom is OSP; with its removal, the amount of Eq. (27) is lesser. In the next step, considering the presence of sensor optimum location obtained in the previous step and updating matrix **PS**, the next optimum location is searched.

4.4 Algorithm D

The basic assumption of this algorithm is that no degree of freedom has any sensor and a sensor is placed in every step of the algorithm. This means that, in every step, one degree of freedom is used for calculating the matrix **PS**. The degree of freedom is OSP; with its attaching, the amount of Eq. (27) is larger. In the next step, when considering the presence of sensor optimum location obtained in the previous step and updating matrix **PS**, the next optimum location is searched.

4.5 Algorithm E

When the elliptical noise in damage space is small, the volume of elliptical noise in response space is large as follows:

$$F_E = \prod_{i=1}^{m} \delta_i = \det(\Sigma) \tag{28}$$

The basic assumption in this algorithm is that every degree of freedom has a sensor and a sensor is removed in every step of the algorithm. The degree of freedom is OSP; with its removal, the amount of Eq. (28) is lower. In the next step, when considering the presence of sensor optimum location obtained in the previous step and updating matrix **PS**, the next optimum location is searched.

4.6 Algorithm F

The basic assumption of this algorithm is that no degree of freedom has a sensor and in every step of the algorithm, a sensor is placed. The degree of freedom is OSP; with its attaching, the amount of Eq. (28) is larger. In the next step, when considering the presence of sensor optimum position obtained in the previous step and updating matrix **PS**, the next optimum location is searched.

5. NUMERICAL EXAMPLES

In this section, the different OSP algorithms presented above were tested for damage detection on a two-dimensional truss in two states, one using the elliptical noise before regularization, another using the equivalent elliptical noise for geometrical viewpoint. This truss as shown in Figure 5, has been previously studied by Bakhtiari-Nejad et al. [14]. The truss was made from steel with $20MP$ elastic modulus and the sections of its elements are according to Table 1. In this study, the damage is detected by the parameter subset selection method. One method to solve the problem in Eq. (9) is to select a single subset of the parameters for updating. The parameter subset selection is a method that selects the best subset of parameters for a candidate set, utilizing some application-dependent cost function that provides a measure of integrity of each subset [22]. The different OSP algorithms and the damage detection method are implemented using the MATLAB software [23]. The standard deviation is the exact criterion for indicating the scatter in the parameters, so

algorithms C and D, which are based on the standard deviation, are the criterion for OSP. Therefore, the results obtained from other algorithms are compared with those algorithms.

Table 1: Cross-sectional areas of two-dimensional truss elements

Element No	Cross-sectional area (cm^2)
1-6	18
7-12	15
13-17	10
18-25	12
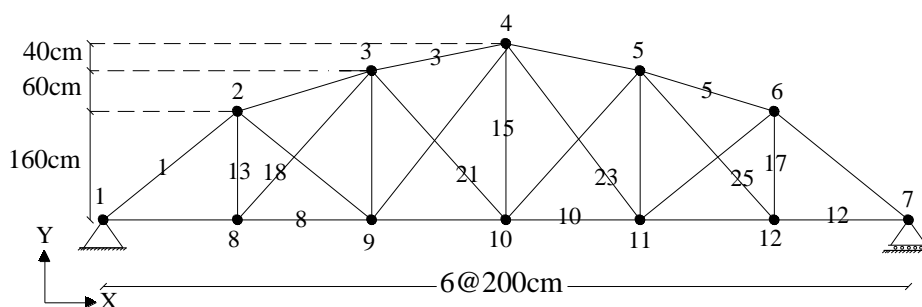
Figure 5. Geometry of two-dimensional truss

5.1 Numerical example 1: Truss under static load

The truss is under static load, according to Figure 6. All results for the 9 sensor locations are listed and compared for states 1 and 2 in Tables 2 and 3, respectively. In these Tables, for example, positions 15 and 18 indicate that the sensor should be placed in the freedom degree of the 9th node in Y-direction and that of the 11th node in X-direction.

Figure 6. Applied static loading

Table 2: Comparison of the optimal sensor locations in state 1

Algorithm	Optimal sensor locations								
A	18	5	20	3	1	7	9	11	12
B	3	15	19	6	8	16	11	18	21
C	18	5	3	20	1	7	9	12	11

D	18	5	20	3	1	7	9	11	12
E	18	5	7	3	9	20	11	12	1
F	18	5	1	7	20	12	9	3	2

Table 3: Comparison of the optimal sensor locations in state 2

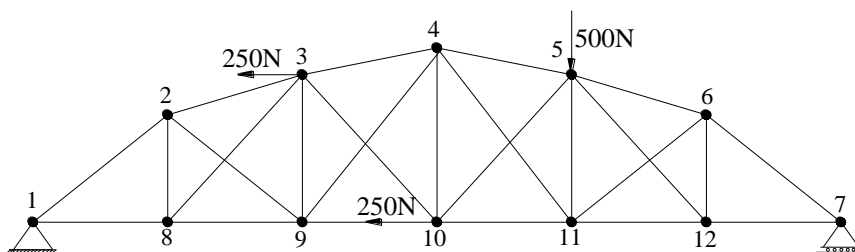| Algorithm	Optimal sensor locations								
A	15	21	10	4	6	17	8	19	2
B	15	8	10	4	17	2	19	14	16
C	15	21	6	10	4	8	17	19	2
D	15	4	21	10	6	17	8	19	2
E	8	19	6	17	21	10	15	4	13
F	15	21	6	19	8	17	4	13	16

To find the best algorithm, three damaged scenarios are considered as shown in Table 4. With recording the displacement of the freedom degrees, where a sensor exists, the sensitivity matrix is calculated then the damage is detected, using the method mentioned, and the results are compared. The results of damage detection in states 1 and 2 are reported in Tables 5-7 and Tables 9-11, respectively.

Table 4: Damaged scenarios

Scenario	Element	Damage percent (%)
1	15	25
	22	25
2	10	15
	18	15
	19	10
3	2	15
	15	15
	17	15
	25	15

Table 5: Comparison of the damage detection in state 1 for scenario 1

Element	Damage percent					
	A	B	C	D	E	F
15	7.15	0	7.15	7.15	7.15	0
22	35.38	37.08	35.38	35.38	35.38	37.27

Table 6: Comparison of the damage detection in state 1 for scenario 2

Element	Damage percent					
	A	B	C	D	E	F
10	17.74	17.49	17.74	17.74	17.74	17.45
18	24.52	13.68	24.52	24.52	24.52	0

| 19 | 0 | 0 | 0 | 0 | 0 | 11.29 |

It is observed that damage detection in state 2 is more accurate, so the purposed filter factor is effective in the algorithms, frequently. The numbers of healthy elements are wrongly detected to be damaging are given in Tables 8 and 12 and it is shown that the numbers are lower in state 2 in the algorithms.

Table 7: Comparison of the damage detection in state 1 for scenario3

Element	Damage percent					
	A	B	C	D	E	F
2	17.52	0	17.52	17.52	17.52	17.5
15	17.45	22.8	17.45	17.45	17.45	17.62
17	0	1145	0	0	0	0
25	21.74	11.01	21.74	21.74	21.74	21.94

Table 8: The number of healthy elements which are wrongly detected to be damaging in state 1

Scenario	Number of healthy element wrongly detected to be damaging					
	A	B	C	D	E	F
1	2	1	2	2	2	2
2	1	2	1	1	1	2
3	0	2	0	0	0	1

Table 9: Comparison of the damage detection in state2 for scenario 1

Element	Damage percent					
	A	B	C	D	E	F
15	30.68	30.39	30.68	30.68	30.61	31.31
22	29.61	29.51	29.61	29.61	29.66	29.67

Table 10: Comparison of the damage detection in state 2 for scenario 2

Element	Damage percent					
	A	B	C	D	E	F
10	17.06	16.84	17.06	17.06	17.04	16.65
18	19.2	14.67	19.2	19.2	18.41	19.69
19	7.32	0	7.32	7.32	6.23	0

Table 11: Comparison of the damage detection in state 2 for scenario 3

Element	Damage percent					
	A	B	C	D	E	F
2	17.74	0	17.74	17.74	9.69	18.47
15	18.6	0	18.6	18.6	16.9	20.09

| 17 | 8.82 | 0 | 8.82 | 8.82 | 0 | 0 |
| 25 | 12.72 | 0 | 12.72 | 12.72 | 0 | 7.65 |

Table 12: The number of healthy elements which are wrongly detected to be damaging in state2

Scenario	Number of healthy element wrongly detected to be damaging					
	A	B	C	D	E	F
1	0	0	0	0	0	1
2	0	1	0	0	0	1
3	0	3	0	0	2	1

The comparison between the results of damage detection in state 1 showed that the damage detection using the measurement locations obtained of algorithms A and E are the best and in state 2, algorithm A is the best. Finally, the results of damage detection obtained from the best algorithms in states 1 and 2 are compared for three damaged scenarios as shown in Figure7. As it can be seen, the best algorithm in state 2 offers better sensor locations and subsequently results in more exact damage detection and the number of healthy elements which are wrongly detected to be damaging is lower in this algorithm.
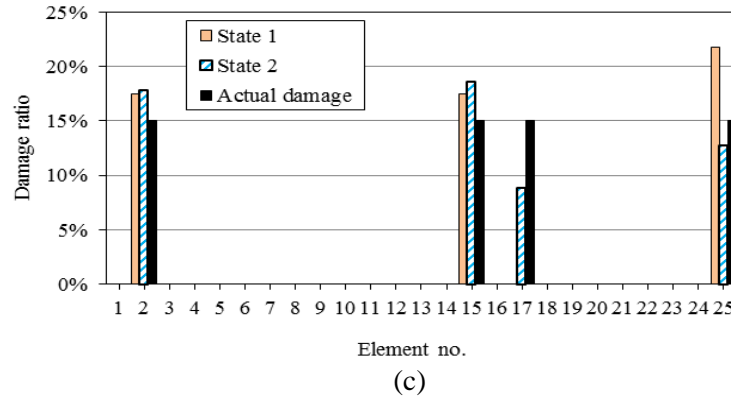

(a)

(b)

(c)
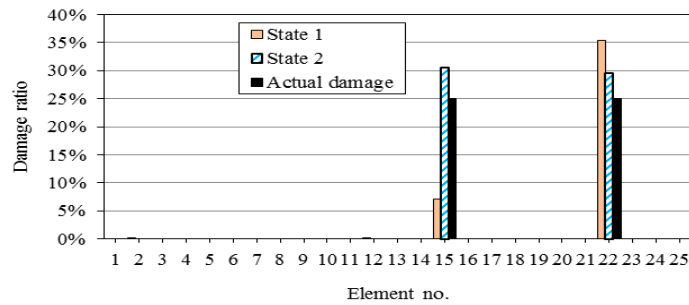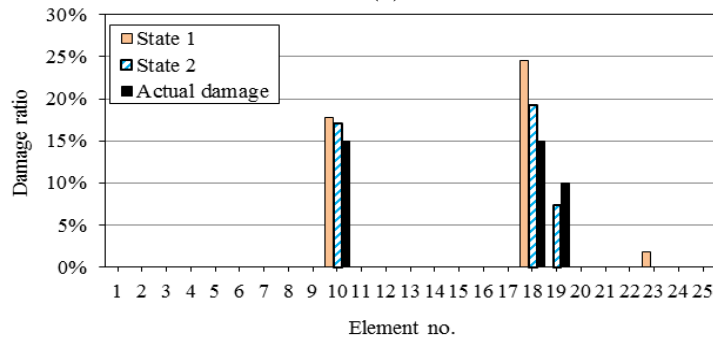
Figure 7. Comparison of the damage detection obtained from states 1 and 2 in (a) scenario 1
(b) scenario 2 (c) scenario 3

5.2 Numerical example 2: Truss under dynamic load

The excitation acting on the truss is a triangular impulsive force with 320.4 *N* peak values
and it lasts for 0.005 *s*. It is applied vertically at node 5. The optimal sensor locations are
obtained for 5 sensors by algorithms in two states. The results are given in Tables 13 and 14,
respectively.

Table 13: Comparison of the optimal sensor locations in state 1

Algorithm	Optimal sensor locations				
A	17	2	12	7	8
B	17	2	7	12	6
C	17	2	7	12	6
D	17	2	12	7	8
E	17	2	12	7	5
F	17	2	7	12	6

Table 14: Comparison of the optimal sensor locations in state 2

Algorithm	Optimal sensor locations				
A	8	19	17	6	21
B	8	19	17	7	6
C	8	19	17	7	16
D	8	19	17	6	21
E	8	10	6	5	11
F	8	7	17	6	20

Three damaged scenarios are considered as shown in Table 15. With recording the
acceleration at the freedom degrees with sensors existing for duration of 0.25 *s*, damage is
detected and the obtained results are compared. The results of damage detection are
reported in Tables 16-18 and Tables 20-22. The numbers of healthy elements are wrongly

detected as damaged, are given in Tables 19 and 23.

Table 15: Damaged scenarios

Scenario	Element	Damage percent (%)
1	2	30
	12	40
3	6	20
	7	30
	8	30
2	5	20
	8	50
	18	20

Table 16: Comparison of the damage detection in state 1 for scenario 1

Element	Damage percent					
	A	B	C	D	E	F
2	0	0	0	0	0	0
12	27.34	27.14	27.14	27.34	34.91	27.14

Table 17: Comparison of the damage detection in state 1 for scenario 2

Element	Damage percent					
	A	B	C	D	E	F
6	15.94	2.98	2.98	15.94	10.29	2.98
7	39.75	19.8	19.8	39.75	40.98	19.8
8	0	0	0	0	0	0

Table 18: Comparison of the damage detection in state 1 for scenario 3

Element	Damage percent					
	A	B	C	D	E	F
5	16.79	14.59	14.59	16.79	13.21	14.59
8	0	0	0	0	0	0
18	0	0	0	0	0	0

Table 19: The number of healthy elements which are wrongly detected to be damaging in state 1

Scenario	Number of healthy element wrongly detected to be damaging					
	A	B	C	D	E	F
1	2	2	2	2	3	2
2	4	5	5	4	5	5
3	4	4	4	4	4	4

Table 20: Comparison of the damage detection in state 2 for scenario 1

Element	Damage percent					
	A	B	C	D	E	F
2	38.96	26.79	27.29	38.96	11.21	17.21
12	44.19	23.87	24.62	44.19	10.86	9.03

Table 21: Comparison of the damage detection in state 2 for scenario 2

Element	Damage percent					
	A	B	C	D	E	F
6	29.74	17.35	20.09	29.74	19.92	17.36
7	28.97	16.8	18.07	28.97	21.98	15.61
8	27.85	31.71	22.44	27.85	20.54	30.99

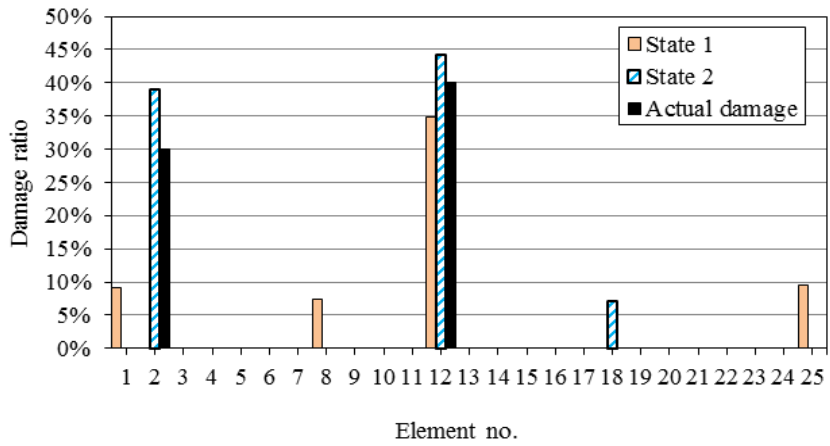Table 22: Comparison of the damage detection in state 2 for scenario 3

Element	Damage percent					
	A	B	C	D	E	F
5	25.74	23.23	28.87	25.74	28.29	16.12
8	54.48	0	0	54.48	0	0
18	32.74	39.92	38.02	32.74	0	28.17

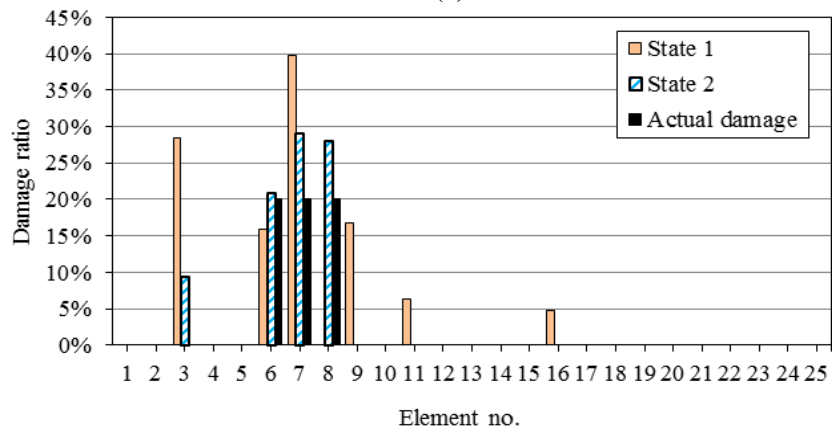Table 23: The number of healthy elements which are wrongly detected to be damaging in state 2

Scenario	Number of healthy element wrongly detected to be damaging					
	A	B	C	D	E	F
1	1	1	1	1	2	1
2	1	2	2	1	1	2
3	1	1	2	1	3	2

The comparison between the results of damage detection in state 1 showed that the damage detection using the measurement locations obtained from algorithms A and E are the best and in state 2, algorithm A is the best.
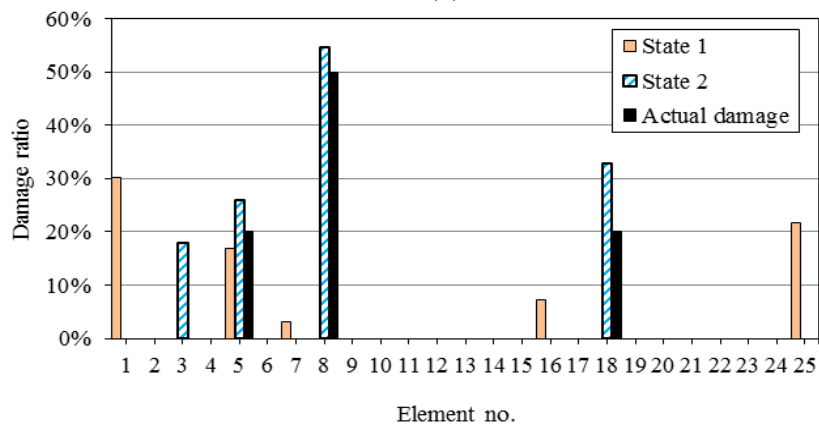
Finally, the results of damage detection obtained from the best algorithms in states 1 and 2 are compared with three damaged scenarios as shown in Figure 8.

(a)

(b)

(c)

Figure 8. Comparison of the damage detection obtained from states 1 and 2 in (a) scenario 1 (b) scenario 2 (c) scenario 3

As it can be seen, the best algorithm in state 2 offers better sensor locations and

subsequently more exact damage detection and the number of healthy elements which are wrongly detected to be damaging is lower in this algorithm. From the results given in this paper, it can be seen that the new geometrical viewpoint is effective for OSP. Generally, the present method is simple and has relatively high accuracy.

6. CONCLUSION

A methodology for sensor placement optimization based on a new geometrical viewpoint is developed in this paper. The view of this method to the OSP is a projection of the elliptical noise on the faces of the response space. Based on this viewpoint, six simple forward algorithms are introduced. The elliptical noise regularized by a filter factor is called equivalent elliptical noise. The damage is detected using the responses record of optimal sensor placements obtained from the algorithms in two states, one using the elliptical noise before regularization, another using the equivalent elliptical noise based on geometrical viewpoint in algorithms. The results as shown state that the algorithm A, based on the norm of the projection of the elliptical noise on face of the response space in state 2, is the best algorithm and the damage detection is more accurate and the number of healthy elements which are wrongly detected to be damaged is lower. So the geometrical viewpoint can be applied to the OSP problem and obtaining optimal placements are better using regularization by the purposing filter factor. It is also shown through the numerical examples that the present method is exact and effective.

REFERENCES

1. Li HN, Yi TH, Yi XD, Wang GX. Measurement and analysis of wind-induced response of tall building based on GPS technology, *Adv Struct Eng*, 2007; **10**: 83-93.
2. Housner GW, Bergman LA, Caughey TK, Chassiakos AG, Klaus RO, Masri SF, Skelton RE, Soong TT, Spencer BF, Yao JTP. Structural control: past, present, and future, *J Eng Mech*, 1997; **123**: 897-971.
3. Li DS, Fritzen CP, Li HN. MinMAC algorithm and comparison of sensor placement methods, *Proceedings of the Conference and Exposition on Structural Dynamic (IMAC '06)*, Orland, USA, 2008, pp. 1-18.
4. Yi TH, Li HN, Gu M. Optimal sensor placement for health monitoring of high-rise structure based on genetic algorithm, *Math Probl Eng*, 2011; doi:10.1155/2011/395101.
5. Inman DJ, Farrar CR, Junior VL, Junior VS. *Damage Prognosis for Aerospace*, John Wiley and Sons, Chichester, UK, 2005.
6. Lie W, Gao WC, Sun Y, Xu MJ. Optimal sensor placement for spatial lattice structure based on genetic algorithms, *J Sound Vib*, 2008; **317**:175-89.
7. Li ZN, Tang J, Li QS. Optimal sensor locations for structural vibration measurements, *Appl Acoust*, 2004; **65**: 807-18.
8. Worden K, Burrows AP. Optimal sensor placement for fault detection, *Eng Struct*, 2001; **23**: 885-901.

9. Kang F, Li JJ, Xu Q. Virus coevolution partheno-genetic algorithms for optimal sensor placement, *Adv Eng Informat*, 2008;**22**:362-70.
10. Sànchez-Montanes MA, Pearce TC. Fisher information and optimal odor sensors, *Neurocomputing*, 2001;**38-40**:335-41.
11. Singh NG, Joshi M. Optimization of location and number of sensors for structural health monitoring using genetic algorithm, *Mater Forum*, 2009;l **33**:359-67.
12. Shah PC, Udwadia FE. A methodology for optimal sensor location for identification of dynamic system, *Appl Mech*, 1978;**45**:188-96.
13. Naseralavi SS, Salajegheh J, Salajegheh E, Fadaee MJ. An improved genetic algorithm using sensitivity analysis and micro search for damage detection, *Asian J Civil Eng*, 2010; **11**: 717-40.
14. Bakhtiari-Nejad F, Rahai A, Esfandiari A. A structural damage detection method using static noisy data, *Eng Struct*, 2005**; 27**:1784-93.
15. Papadimitriou C. Optimal sensor placement methodology for parametric identification of structural systems, *J Sound Vib*, 2004; **278**: 923-47.
16. Guo HY, Zhang L, Zhang LL, Zhou JX. Optimal placement of sensors for structural health monitoring using improved genetic algorithms, *Smart Mater Struct*, 2004;**13**: 528-34.
17. Naorem GS, Joshi M. Strategy for health monitoring of bridge superstructure, *Proceedings of the national Conference on Advances in Bridge Engineering*, IIT, India, 2006.
18. Said WMI, Staszewski WJ. Optimal sensor location for damage detection using mutual information, *Proceedings of the 11th International Conference on Adaptive Structures and Technologies (ICAST)*, Nagoya, Japan, 2000, pp. 428-35.
19. Perez RE, Behdinan K. Particle swarm approach for structural design optimization, *Comput Struct*, 2007**; 85**: 1579-88.
20. Li XY, Law SS. Adaptive Tikhonov regularization for damage detection based on nonlinear model updating, *Mech Syst Signal Process*, 2010; **24:** 1646-64.
21. Weber B, Paultre P, Proulx J. Consistent regularization of nonlinear model updating for damage identification, *Mech Syst Signal Process*, 2009; **23**: 1965-85.
22. Friswell MI, Mottershead JE, Ahmadian H. Combining subset selection and parameter constraints in model updating, *J Vib Acoust*, 1998; **120**: 854-59.
23. MATLAB, Version 7.10.0. *MATLAB Optimization Toolbox User's Guide*, The Math Works, 2010.